International Journal of Mechanical, Industrial and Aerospace Sciences
ISSN: 2517-9950
Vol:1, No:2, 2007

A parametric Study of an Inverse Elastostatics Problem (IESP) using Simulated Annealing, Hooke & Jeeves and Sequential Quadratic Programming in conjunction with Finite Element and Boundary Element Methods

Ioannis N. Koukoulis, Clio G. Vossou, and Christopher G. Provatidis

Abstract**—**The aim of the current work is to present a comparison among three popular optimization methods in the inverse elastostatics problem (IESP) of flaw detection within a solid. In more details, the performance of a simulated annealing, a Hooke & Jeeves and a sequential quadratic programming algorithm was studied in the test case of one circular flaw in a plate solved by both the boundary element (BEM) and the finite element method (FEM). The proposed optimization methods use a cost function that utilizes the displacements of the static response. The methods were ranked according to the required number of iterations to converge and to their ability to locate the global optimum. Hence, a clear impression regarding the performance of the aforementioned algorithms in flaw identification problems was obtained. Furthermore, the coupling of BEM or FEM with these optimization methods was investigated in order to track differences in their performance.

Keywords**—** Elastostatic, inverse problem, optimization.

I. Introduction

INVERSE analysis is the general name given to problems where not all of the information, that is required to analyze the system, is known a priori, meaning that they may not be classified as direct problems. A direct problem involves the determination of the response of a system given the domain of the problem and its boundaries, the governing laws or equations, and the boundary conditions.

In the case of IESP of internal flaw detection, the boundaries of the flaw are not known. In order to analyze this kind of problem, a static response is obtained, under known boundary conditions. Solving this problem directly is not possible unless it is considered as an optimization task.

Optimization is the search of the minimum or maximum of a function that is commonly referred to as cost or objective function. This function is dependent on the design variables, which are the unknown system parameters. The objective of the optimization process is to determine the values of these design variables that minimize or maximize the cost function. In addition to optimizing the objective function, the design has to meet certain criteria or specifications which may be represented mathematically by constraint equations [1].

In the case of IESP, the identification process takes an initial guess for the flaw shape and location, the displacements are obtained at the selected points and the error, due to the guessed flaw, is computed. The flaw shape and location that minimizes the error is found giving an approximation to the actual flaw [2].

The two methods used for the determination of the displacements are the finite element (FEM) and the boundary element (BEM) methods, which are the mostly used CM. The standard FEM equation for static analysis is: $\mathbf{K}(z)\cdot\mathbf{u}(z)=\mathbf{f}(z)$ where **K** is the assembled global stiffness matrix, **u** is the nodal displacement vector, and **f** is the nodal force vector. More details can be found in [3].

Respectively, the standard BEM equation for static analysis is: $\mathbf{G}(z)\cdot u(z)=\mathbf{H}(z)\cdot t(z)$ where vectors **u** and **t** include all boundary displacements and tractions and **G** and **H** are suitable influence matrixes. Theoretical details about the BEM can be found, among others, in [4].

In both CM, the vector z includes all the design variables which are required for the determination of the considered circular flaw.

The FEM is a well-established procedure for structural analysis and formed the basis of most early inverse methods. On the other hand, the BEM has become a popular alternative, possessing many advantages over the FEM [2].

The IESP of flaw detection, using boundary response measurements under a prescribed loading, has been encountered in several previous works. Different test cases and optimization methods (OM) have been tested. In 2D cases of one circular defect, neural networks have been applied [5].

Manuscript received February 21, 2007. This work is co-funded by the European Social Fund (75%) and National Resources (25%) - Operational Program for Educational and Vocational Training II (EPEAEK II) and particularly the Program PYTHAGORAS.

I. N. Koukoulis, is with the School of Mechanical Engineering, National Technical University of Athens, GR-15773 Athens, Greece (e-mail: jkouk@mail.ntua.gr).

C. G. Vossou is with the School of Mechanical Engineering, National Technical University of Athens, GR-157 73 Athens, Greece (e-mail: cvossou@central.ntua.gr).

C. G. Provatidis is with the School of Mechanical Engineering, National Technical University of Athens, 9 Iroon Polytechniou Avenue, GR-15773 Athens, Greece (phone: +30-210-7721520; fax: +30-210-7722347; e-mail: cprovat@central.ntua.gr).

The same OM has been tested also in the case of a unique crack in a plate [6]. [7] used genetic algorithms to detect three circular or elliptical defects in a plate. Genetic algorithms were also implemented in the work of [8] for the identification of 3D ellipsoidal defects in a cube and a circular defect in an L-profiled structure. In 3D structures, distributed evolutionary algorithms were used, for example by [9]. The performance of quasi Newton optimization methods for unconstrained optimization, namely Gauss-Newton, Levenberge-Marquarant and BFGS, has been compared in [10] who used, among others, the test case proposed by [11]. Steepest Descent and BFGS Quasi Newton methods have been also used in [12] for the identification of a circular or ellipsoid flaw in a cylinder. Finally, [1] used the SQP in crack propagation problems, not covered in this paper.

II. Optimization Algorithms

The OMs tested in this paper belong to three different categories of optimization algorithms. The first one is Simulated Annealing (SA) which is a stochastic algorithm, the second is Hooke & Jeeves (HJ) which is a pattern search algorithm and the last one is Sequential Quadratic Programming (SQP) which is an effective deterministic algorithm that has been already used in inverse problems [1,13]. In turn, the implementation of SQP is included in MATLAB Optimization Toolbox, HJ has been implemented according to [14] and the implementation of SA is included in MATLAB functions of the MathWorks site [15, 16].

Among the tested optimization algorithms, SQP is the only one that can inherently encounter constraints, so linear constrains provided design vectors with a physical meaning. The other two methods are designed for unconstrained problems. However, their use can also be extended for solving constrained problems if the imposed limitations are appropriately implemented to the quantity to be optimized. This task may be accomplished through a penalization method, where the constraints are introduced into the objective function in a weighted manner through a penalty. Towards this direction, in the current work a very simple scheme was used; if either a small or a large constraint violation occurred then the objective function obtained a very high value. This was a hard penalization that pushed the examined algorithms to their limits. A brief description for each algorithm follows.

A. Simulated Annealing

Simulated Annealing is a Monte Carlo approach introduced by Kirckpatrick et al. in 1983. The term *simulated annealing* derives from the roughly analogous physical process of heating and then slowly cooling a substance to obtain a strong crystalline structure. In simulation, a minimum of the cost function corresponds to the ground state of the substance. The SA process lowers the temperature by slow stages until the system "freezes" and no further changes occur. At each temperature the simulation must proceed long enough for the system to reach a steady state or equilibrium. The sequence of temperatures and the number of iterations applied to thermalize the system at each temperature comprise an annealing schedule.

To apply SA, the system is initialized with a particular configuration. A new configuration is constructed by imposing a random displacement. If the energy of this new state is lower than that of the previous one, the change is accepted unconditionally and the system is updated. If the energy is greater, the new configuration is accepted probabilistically. The probability of accepting such a configuration is given by Boltzmann's probability distribution function $p(\Delta E) = e^{-\frac{\Delta E}{T}}$ where T is the temperature and ΔE is the change in the energy function. This is the Metropolis step, the fundamental procedure of SA. This procedure allows the system to move consistently towards lower energy states, yet still avoid local minima due to the probabilistic acceptance of some upward moves. It uses T (temperature) and the size of the downhill move in a probabilistic manner. The smaller T and the size of the uphill move are, the more likely that move will be accepted.

The SA algorithm is implemented as described below:

1. Values for the initial temperature T (1E-01), the number of function evaluations for constant temperature K_{max} (70), the maximum number of successful tries for constant temperature (30) and the maximum number of consecutive rejections (1000) are set.
2. Evaluate the function at a starting point f_{min}
3. Set K=K+1.
4. Generate a new point randomly and evaluate f_s.
5. Compare f_s to f_{min}

5.1 If $f_s < f_{min}$ then accept the move and set $f_s = f_{min}$.

5.2 If $f_s > f_{min}$ accept the uphill moves according to the Metropolis criteria.

5.2.1 If the move is accepted, the algorithm moves on from that point.

5.2.2 If the move is rejected, another point is chosen instead for a trial evaluation.

6. Check for convergence (T_{min}=1E-07 or 'Maximum consecutive rejections or Maximum number of Success) and either go to step 3 or go to 7.
7. If K less than K_{max} go to 3, else go to 8.
8. A decrease in the temperature is imposed according to cooling schedule ($T=0.8*T$).
9. Check for convergence (T_{min}=1E-07 or Maximum consecutive rejections or Maximum number of Success) and either go to step 3 or Stop.

B. Hooke & Jeeves

Hooke and Jeeves introduced their algorithm 1961. It is a direct search method that requires no derivatives of the objective function but only function evaluations. The standard Hooke & Jeeves pattern search algorithm consists of one-variable-at-a-time exploratory moves about a base point solution to determine an appropriate direction of search (pattern). Following the exploratory search, a series of pattern moves are made to accelerate the search in the direction determined in the exploratory search. Exploratory searches and pattern moves are repeated until a termination criterion is met. For the purposes of this paper, the implementation of Hooke & Jeeves algorithm according to Belegundu et al [14] has been used. A very brief description is given below.

1. Search initiation from a given point B with coordinates $\vec{x}_B$.
2. *Exploration* about point B with step s (0.8).
2.1 If exploration about base point not successful, step *s* is reduced (multiplication by 0.5).
2.2 If exploration successful, the pattern direction BP is established as $(x_P\text{-}x_B)$.
3. P is considered as new base point and is renamed as B. Original point B renamed as B'.
4. BB' extended along the pattern direction to point E. $(x_E=2x_B\text{-}x_{B'})$.
4.1 Exploration is performed about point E.
4.2 If exploration about base point not successful, step *s* is reduced.
4.3 If exploration successful new pattern direction BE is established as $(x_E\text{-}x_B)$
5. If s < 1E-08 then stop.

C. Sequential Quadratic Programming (SQP)

SQP is a second order method for constrained problems and consists of three main stages:

1. Updating the Hessian matrix of the Lagrange function
2. Quadratic Programming Solution
3. Line Search and merit function calculation

Given the description in the general problem, the principal idea is the formulation of a quadratic subproblem based on a quadratic approximation of the Lagrangian function

$$L(x,\lambda)=f(x)+\sum_{i=1}^{m}\lambda_i.g_i(x)$$

where λ are the Lagrangian coefficients and g are the problem constraints.
The maximum number of iterations and function evaluations is 100 and 1000, respectively. Concerning the tolerance on linear constrains and cost function a common value of 1E-10 was set. The corresponding tolerance on the design variables is set to 1E-6.

III. Description of the Test Case

A plane strain square plate with one circular flaw is considered as in Fig. 1. The material constants are the shear modulus G = 1E+05 and Poisson's ratio v = 0.30. The dimension of the side of the plate is L = 10, all in compatible units. Moreover, the right-hand side external boundary (bc) is fixed in both directions and the loading is applied on the left-hand side external boundary (ad) as well as on the bottom one (ab) as pressure with a value equal to 1000, in the horizontal Ox and in the vertical Oy coordinate direction, respectively. Pressure loading is selected instead of tension since it is thought that it results in a more difficult situation. The circular flaw can be in five different locations and can have five different radius dimensions as shown in Fig. 1. The five different center locations have coordinates 1(2.50,2.50), 2(2.50,7.50), 3(2.50,7.50), 4(5.00,5.00), 5(7.50,7.50) and the different radius dimensions are 0.20, 0.40, 0.60, 0.80 and 1.00 [17].

Concerning the possible location and size of the flaw, the above data was selected so as to be representative. In more details, the locations of the flaw are selected in order to investigate the effect of a variation in size of the artifact close to a corner with different boundary conditions, or in the center were the influence of the boundary conditions is reduced. Using this data, 25 different test cases have been constructed.

For the BEM analysis, the boundaries of the plate are discretized by means of quadratic boundary elements. In all examples presented here, the external boundary is discretized by means of 40 boundary elements (i.e. a total of 80 nodes) and the circular flaw is discretized by means of 8 boundary elements (i.e. additional 16 nodes).

On the other hand, for the FEM analysis quadratic triangular elements were used. The FEM mesh was created with 20 element divisions per side and free mesh (i.e. about 3600 nodes in total and 1700 elements) and only the results at the edge nodes were taken under consideration so as to have the same number of data as in the BEM model. The FEM model has obviously a finer mesh since this ensured a satisfactory quality of results and stability (Fig. 2).

For the formulation of the identification problem as an optimization process, as design variables the spatial coordinates of the centre of the circular flaw (x,y) and its radius r were considered. Furthermore, the cost function is defined as

$$f(u)=1000+ln\left(10^{-6}+\sum_{side}\left(\frac{\sum(\Delta u_x)^2}{\left(max\left(u_x^{real}\right)^2\right)}+\frac{\sum(\Delta u_y)^2}{\left(max\left(u_y^{real}\right)^2\right)}\right)\right)$$

where Δu_i is the difference between the calculated displacement on ith direction $\Delta u_i^{calculated}$, while u_i^{real} are the corresponding experimental data [6].

The design variables are used in an automatic procedure to create a suitable mesh for the flaw, and the displacements u are calculated at the free boundaries (ab, cd, da) as shown in Fig. 1.

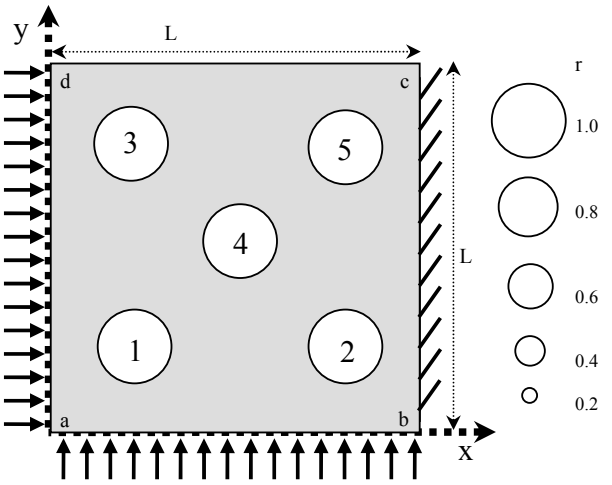

Fig. 1 Geometry and boundary conditions of the test cases

The design variables corresponding to the center coordinates were chosen to lie in the interval of [0.5, 9.5] and the radius in [0.1, 2.0]. In this manner, the imposed constraints have a physical meaning, as the flaw specified by the design variables is ensured to lie completely inside the plate.

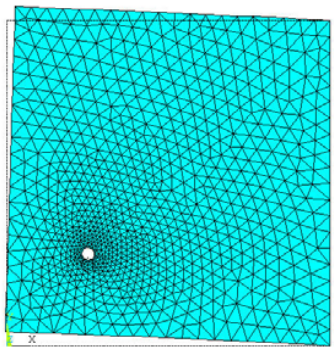

Fig. 2 FE mesh for the center at 1 (2.50,2.50) and radius 0.20

For each of the three abovementioned optimization methods, the IESP has been solved for 100 times. The problem was solved one time for each location of circular flaw with the five different radii, with four different starting points. As initial vector for the optimization algorithms, the location of one of the flaws 1-5 Fig. 1 (excluding the one that coincides with the flaw to be detected) and the radius of 0.50 is used.

IV. Results

The IESP has been solved by both the computational methods for the direct problem (i.e. BEM, FEM). In Table I the percentage of "successful runs" for each combination of OM and CM, with at least one initial vector, is presented. By the term "successful run" the calculation of the design variables with an error less than 0.5% is meant.

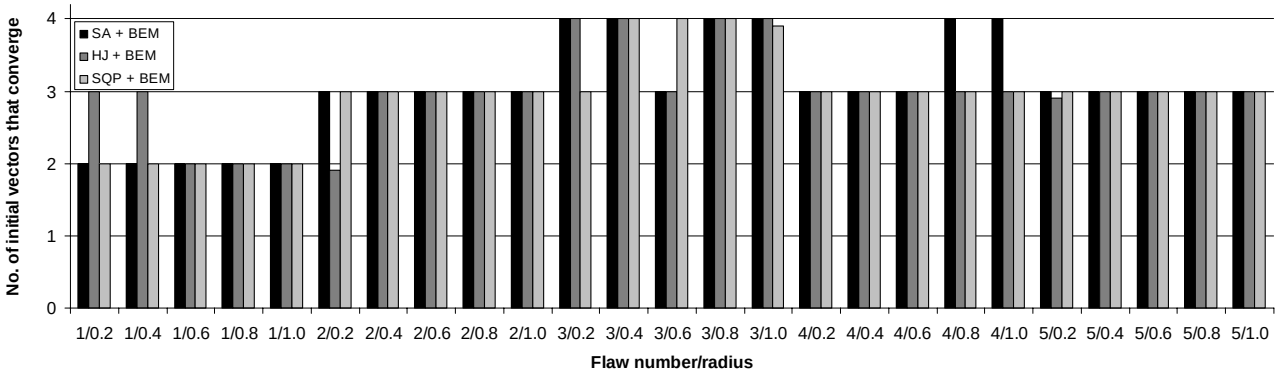

Fig. 3 OMs convergence in terms of initial vector and flaw number / radius (BEM)

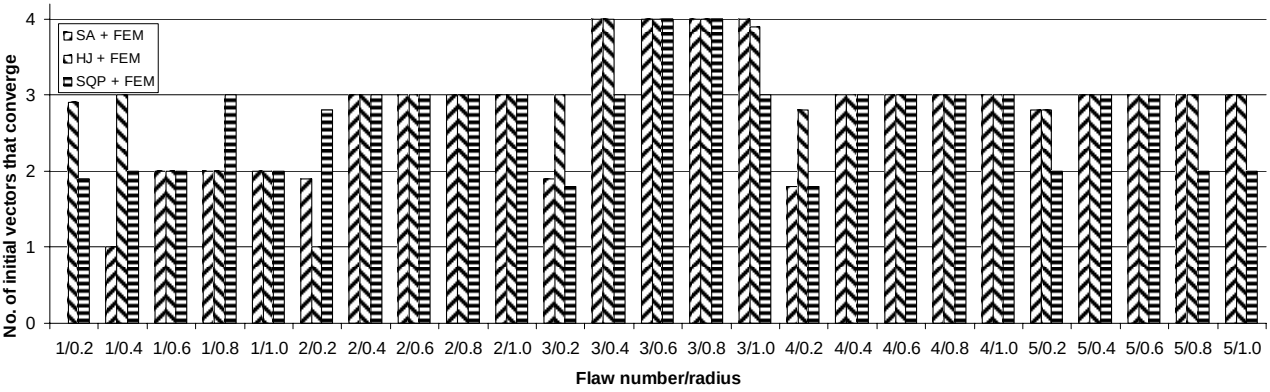

Fig. 4 OMs convergence in terms of initial vector and flaw number / radius (FEM)

TABLE I
The Percentage of "Successful Runs" for each Combination of OM and CM, with at Least one Initial Vector

OM + CM	% of successful runs
SA + FEM	68
SA + BEM	76
SQP + FEM	68
SQP + BEM	74
HJ + FEM	74
HJ + BEM	75

In Fig. 3 and 4 the performance of each optimization method per final point in terms of successful runs, is shown for BEM and FEM, respectively. Every successful run was counted as 1, only if the error of the convergence to the final point was less than 0.2%. If the error was higher, but less than 0.5%, it was counted as 0.9. The distinction was made in order to show the ability of every combination OM and CM to converge at the exact global optimum.

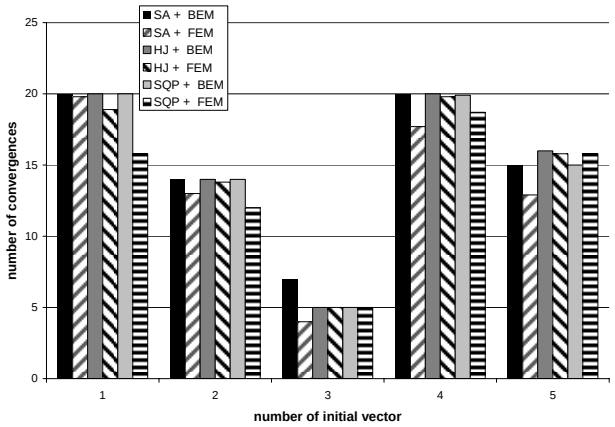

Fig. 5 Number of successful runs per initial vector

In Fig. 5 the number of successful runs per starting vector in BEM and FEM for all the optimization methods is presented.

The average number of function evaluation per initial vector is shown in Fig. 6. Finally, for reasons of thoroughness, the convergence histories are presented for each OM for both FEM and BEM using SA, HJ and SQP in Fig. 7, 8 and 9 respectively. The presented results concern a typical case, center 5 and radius 0.4, in which all the optimization methods converge with both the CM starting from the same starting vector, center 1 and radius 0.5.

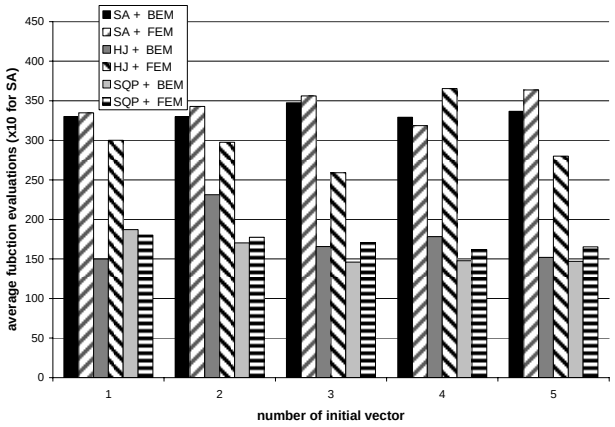

Fig. 6 Number of function evaluations per initial vector

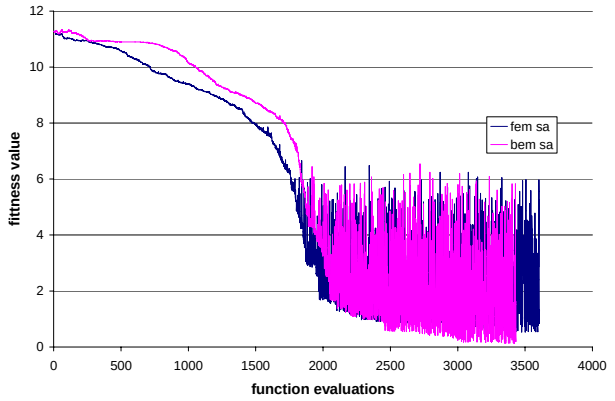

Fig. 7 SA convergence history

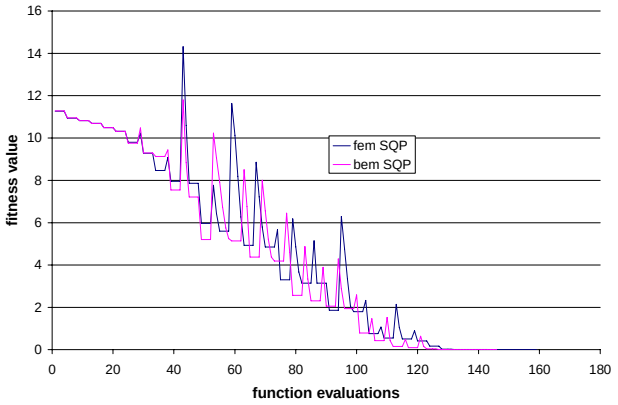

Fig. 8 SQP convergence history

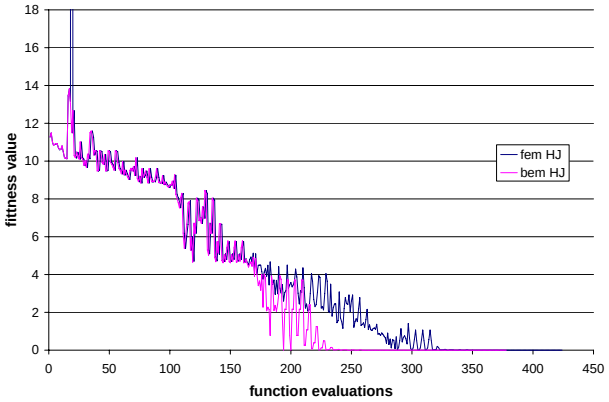

Fig. 9 HJ convergence history

V. Discussion

The interpretation of the results leads to remarks concerning (a) the use of BEM and FEM in inverse problems, (b) the behavior of the optimization methods and (c) general remarks.

Regarding the CM for the solution of the direct problem it is obvious that both FEM and BEM give satisfactory results and are efficient in terms of identifying the location and the size of the circular flaw. As it can be seen in Table I, using BEM all the OM have almost the same percentage of success and approximately 75% but when using FEM the SA and SQP have lower percentage of success (68%) than HJ that remains near the same value. Furthermore, the FEM demands more function evaluations (Fig. 6-9) and at the cases of pretty small circular flaws (r = 0.2) the identification included slight error. This is caused due to the restrictions of meshing which might not be accurate enough to describe small holes.

If the performance of each combination is stated by the fact of reaching the global optimum with at least one of the four initial vectors, then all the combinations are successful except the case SA+FEM where there is one failure for the flaw 1/0.2 (flaw number at the location 1 with radius 0.2) as shown in Fig. 4 where none of the starting vectors lead to a successful history. It is also remarkable that all the OM combined with BEM have at least 2 out of the 4 initial vectors leading to the global optimum. The FEM needs about 20 times more computational time for each analysis than BEM giving a serious advantage to BEM.

In Fig. 6 the average number of function evaluation needed for convergence for every initial vector is shown. The choice of initial vector does not seem to influence the number of function evaluations, though the CM does. BEM tends to need less function evaluations than FEM, especially when using HJ. As far as the difference of the performance of the OM is concerned, it is easy to observe that SA needs more function evaluations since it is a stochastic method. SQP and HJ need more or less the same number of function evaluations when combined with BEM while combined with FEM, HJ needs more than SQP (Fig. 7-9). On the other hand, regardless the CM, even if sometimes SQP converges quicker, in terms of function evaluations this does not mean less CPU time in total since it is a method that needs more computational time than the others in its every iteration.

Observing the figures with the histories of convergence for every method it becomes obvious that, for both CM the cost function value diminishes the same way for much more iterations using HJ than using SQP. These two methods have the same history at first and afterwards they change path due to slight changes on the CM concerning their accuracy and the influence of mesh. Only the SA does not have common path for both CM since it uses a random number generator.

In SA the cost function value at first diminishes quicker for the FEM than the BEM but as the number of evaluations increases the drop rate falls and the BEM converges quicker, though this could not be considered as a rule since the included random number generator plays an important role. SQP and HJ follow more or less the same way independently from the CM but from a point and further the HJ seem to converge more quickly. The different history of each method could be explained by their different nature.

In Figs. 3 and 4 the location and size of each one of the 25 flaws is characterized by the fact of being detected. The location is more important for both CM. Additionally, the size is negligible for BEM, while for FEM only the smallest size (r = 0.2) has fewer successes. The easiest location to be found is the upper left corner (3), the most difficult is the lower left (1) and all the other three seem to be of the same difficulty. A possible explanation is that location 3 is close to an edge with no pressure or support so its result is clearer. On the other hand, the location 1 is close to the two edges that carry the loading, so its result is affected by the boundary conditions.

In Fig. 5 it is shown that the initial vector plays a significant role in the convergence for all the combinations OM and CM. The best initial vector is no. 4, as expected, since it lies in the center of the plate and it has the same distance from all the flaws to be identified. However, this is not the only vector that gives satisfactory results. Vector 1, which is located in the lower left corner, has more or less the same results. If it is also considered that this is the flaw more difficult to identify (Fig. 5), it should be considered as a good starting point. An interesting result is that the initial vector with a center at the location 3 leads to the least successful runs. These two last remarks show that the location which could be considered as good for starting vector is difficult to be located and the opposite.

VI. Conclusion

Comparing FEM with BEM according to their ability regardless the optimization method, BEM is more efficient. Furthermore, this parametric study indicated that the initial vector seems to be more significant in the overall behavior of the optimization methods and computational methods than any other parameter.

As long as the three optimization algorithms are concerned, they are expected to perform in different way and so they are doing. One could say that all the methods solve the problem successfully, with the same accuracy so the only parameter capable of differentiating the method in this test case should be the computational cost and the difficulty of implementation. In these terms, the Hooke and Jeeves algorithm seems to be a promising optimization method in the field of inverse design. Another feature that makes Hooke and Jeeves promising is that it maintains the same satisfactory performance in FEM as well as in BEM.

References

[1] M. S. Gadala and A. D. B. McCullough, “On the finite element analysis of inverse problems in fracture mechanics (Inverse problems in fracture mechanics)”, *Engineering Computations*, vol. 16 No. 4, 1999, pp. 481-502.
[2] S. C. Mellings and M. H. Aliabadi, “Flaw Identification Using The Boundary Element Method”, *International Journal For Numerical Methods In Engineering*, vol. 38, 1995, pp. 399-419.
[3] G. Beer, and J. Q. Watson, *Introduction to Finite Element Methods for Engineers.* Chichester, CA: John Wiley & Sons, 2002.
[4] C. A. Brebbia and J. Dominguez, *Boundary Elements: an introductory course*. New York CA: Computational Mechanics Publications, McGraw-Hill Company, 1992.
[5] M. Tanaka and Y. Masuda, “Boundary element method applied to some inverse problems”, *Engineering Analysis*, vol. 3, 1986, pp. 138-143.
[6] G. E. Stavroulakis and H. Antes, “Nondestructive elastostatic identification of unilateral cracks through BEM and neural networks”, *Computational Mechanics*, vol. 20, 1997, pp. 439–451.
[7] H. Koguchi and H. Watabe, “Improving defects search in structure by boundary element and genetic algorithm scan method”, *Engineering Analysis with Boundary Elements*, vol. 19, 1997, pp. 105-116.
[8] M. Engelhardt, M. Schanz, G. E. Stavroulakis and H. Antes, “Defect identification in 3-D elastostatics using a genetic algorithm”, *Optim Eng*, vol. 7, 2006 pp. 63–79.
[9] T. Burczynski, W. Kus, A. Dlugosza and P. Orantek, “Optimization and defect identification using distributed evolutionary algorithms”, *Engineering Applications of Artificial Intelligence*, vol. 17, 2004, pp. 337–344.
[10] G. Rus and R. Gallego, “Optimization algorithms for identification inverse problems with the boundary element method”, *Engineering Analysis with Boundary Elements*, vol. 26, 2002, pp. 315-327.
[11] L. M. Bezerra and S. Salgal, “A boundary element formulation for the inverse elastostatics problem (iesp) of flaw detection”, *Int. J. For Numerical Methods In Engineering*, vol. 36, 1993, pp. 2189-2202.
[12] S. C. Mellings and M. H. Aliabadi, “Three-Dimensional Flaw Identification Using Inverse Analysis”, *Int. J. Engng Sci*., vol. 34, No. 4, 1996, pp. 453-469.
[13] N. S. Mera, L. Elliott and D. B. Ingham, “Numerical solution of a boundary detection problem using genetic algorithms”, *Engineering Analysis with Boundary Element*s, vol. 28, 2004, pp. 405–411.
[14] A. D. Belegundu and T. R. Chandrupatla, *Optimization concepts and applications in engineering.* New Jersey, CA: Prentice Hall, 1999.
[15] Matlab Optimization toolbox.
[16] Mathworks, http://www.mathworks.com/
[17] N. Tosaka, A. Utani and H. Takahashi, “Unknown defect identification in elastic field by boundary element method with filtering procedure”, *Engineering Analysis with Boundary Elements*, vol. 15, 1995, pp.207-215.